Renewable Energy 252 (2025) 123406

Contents lists available at ScienceDirect

Renewable Energy

journal homepage: www.elsevier.com/locate/renene

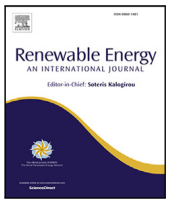

Microalgae bio-reactive façade: Open data for nation-scale production potential assessment☆

Victor Pozzobon

Université Paris-Saclay, CentraleSupélec, Laboratoire de Génie des Procédés et Matériaux, Centre Européen de Biotechnologie et de Bioéconomie (CEBB), 3 rue des Rouges Terres 51110 Pomacle, France

ARTICLE INFO

Dataset link: https://github.com/victorpozzobon/biofacade, https://www.data.gouv.fr/en/datasets/donnees-d-observation-des-principales-stations-meteorologiques/, https://www.statistiques.developpement-durable.gouv.fr/catalogue?page=dataset&datasetId=6513f0189d7d312c80ec5b5b, https://www.insee.fr/fr/information/2114627, https://www.data.gouv.fr/fr/datasets/communes-de-france-base-des-codes-postaux/

Keywords:
Microalgae
Biofaçade
Production
Open data
Nation scale prediction

ABSTRACT

This work combines microalgae culture numerical modeling and open big data from the French weather forecast agency and the French government to evaluate the annual deployment potential for microalgae biofaçade over France's mainland territory. After data curation, three scenarii were evaluated. The annual production potential offered by new buildings (offices, retail buildings, hotels, industrial buildings, and state buildings) lies between +28.9 ± 3.7 and +202.6 ± 17.4 ton per year for the conservative and the optimistic scenario, respectively. It corresponds to producing 6100 to 62,000 microalgae biofaçade units, which is more than enough to sustain year-round continuous production. Analyzing the host building type revealed that retail buildings (*e.g.*, malls) are the most favorable places for the technology, followed by state buildings and offices. Finally, in depth analysis of the results showed that façade orientation is the first predictor of the system performance while its geographical location in France is only a modulator of it.

1. Introduction

Since the middle of the 20th century, humanity is continuously increasing the pressure on its host ecosystem. Over 1971, humans consumed for the first time more than what Earth could provide in a renewable manner over a year [1]. Since then, the situation never stopped worsening. The drivers for this problematic situation are both an increase in number and an improvement in the average quality of life. Among the different compartments of our ecosystem, the most stressed ones might be fossil fuels, water, arable lands, and biodiversity [2]. Mitigating this situation by whichever sustainable means is, therefore, an imperious need. In this context, microalgae emerge as a tool capable of helping humanity reduce its footprint. Indeed, they are able to produce numerous molecules with applications ranging from food and feed [3] to pharmaceutical industries [4,5], and nutraceutics [6] while delivering ecosystemic benefits (CO_2 fixation [7], phosphate fixation [8], nitrogen fixation [9], effluent bioremediation [10] etc.). Finally, extraction process leftovers could be valorized as biofuel [4]. Despite their potential, numerous scientific challenges must be addressed before microalgae can fully deliver on their promises. Among them, reducing the cost of microalgae production is critical.

Cutting costs while not compromising biomass quality can be achieved by massive outdoor deployment of streamlined photobioreactors. With this approach, photobioreactor manufacturing would benefit from the scale cost cutdown of mass production. Furthermore, large-scale operations would generate massive operational feedback, driving best practices sharing and performance gains [11]. Yet, two challenges are to be faced to successfully implement a large-scale outdoor bioprocess. First, the cultures would experience natural light and temperature cycles, making process operation less straightforward than indoors. Second, large areas with adequate sun access would have to be acquired. Fortunately, a microalgae technology addressing part of these limitations exists: the façade-integrated microalgae photobioreactors (biofaçades, in short, and hereinafter) [12,13]. This association represents a building/biotechnology synergy belonging to the emerging concept of advanced architecture (which is broader

☆ Communauté urbaine du Grand Reims, Département de la Marne, Région Grand Est and European Union (FEDER Grand Est 2021-2027) are acknowledged for their financial support to the Chair of Biotechnology of CentraleSupélec and the Centre Européen de Biotechnologie et de Bioéconomie (CEBB)

E-mail address: victor.pozzobon@centralesupelec.fr.

https://doi.org/10.1016/j.renene.2025.123406
Received 30 October 2024; Received in revised form 7 March 2025; Accepted 7 May 2025
Available online 25 May 2025
0960-1481/© 2025 The Author. Published by Elsevier Ltd. This is an open access article under the CC BY-NC license (http://creativecommons.org/licenses/by-nc/4.0/).

than microalgae bio-reactive façade and, for example, encompasses thermal/photovoltaic façades [14]). The synergistic aspects come from the fact that both compartments would benefit from their association. On the photobioreactors side, the benefits would be a reduced production cost as the host building offers vertical support and some utilities (*e.g.*, water and potentially nutrients such as carbon dioxide), and a dampening of the temperature variation thanks to the building thermal inertia. On the building side, gains would be shading, improved thermal comfort by better modulating incident heat [15], pollution emission reduction [16], energy generation [12], and aesthetic enhancements [17].

Still, before massively deploying a technology on a large scale, its potential relevance has to be assessed. To do so, one needs preliminary data, either experimental or numeric, and a methodology to upscale them. In the case of microalgae biofaçade, investigators tackled the knowledge gaps with three methods. Experiments came first. They focused on isolated microalgae biofaçade modules (not integrated into a host building). They delivered answers to basic questions such as thermal performance [18] or biomass productivity [19,20]. Then came numerical models. They widened the scope towards design and integration questions (single vs. double glazing [21,22], façade-integrated vs. double skin [23,24], straight vs. free-form [25]), analyzed the impact of weather [26,27], and delivered insight on visual comfort and aesthetics [15,17]. Finally, a short-lasting yet important, large-scale experiment has to be mentioned: the BIQ house in Hamburg, Germany. For an architecture exhibition, the building was equipped with 185 m^2 of biofaçade [28]. This trial delivered solid measurement of the microalgae photoconversion efficiency (4.4%, comparable to laboratory studies 5.01% [29], 5.65% [30], or 4.34 % [31]), and validated building dwellers acceptation of the technology.

While they delivered insightful knowledge about biofaçade systems, none extrapolated their findings to the national scale. Indeed, such an endeavor requires a proper methodology on top of small-scale performance quantification. The main pitfall to avoid is multiplying small-scale results by a scale ratio factor, incidentally ignoring the numerous hurdles that will arise in real life (weather, implementation location suitability, regulations, etc.) [32]. Most of the studies carrying out large-scale extrapolation of microalgae outdoor processes are dedicated to biofuel production potential assessment. While their focus differs slightly from the one in this article, their findings are worth considering, at least for guidance. Among the different articles, one could note the one of Moody et al. who estimated the lipid production potential using *Nannochloropsis* [32]. Using a model powered by weather data (cloud cover, temperature, etc.) from 4388 stations worldwide, they have been able to map the production potential worldwide. Diving in-depth into their results, they showed that not accounting for temperature impact on cell metabolism could lead to an overestimation by a factor of two. In the same way, cloud cover has been shown to be a strong modulator of this microalgal bioprocess. In the same year, Coleman et al. reported an investigation of US Gulf Coast biodiesel production potential [33]. In their demonstration, the authors underlined that it is paramount to account for weather and to do this over several years (30 in their case) and at multiple locations. Indeed, assuming maximum productivity all year long is nonsense, yet designing a process based on the average production over a single year is also a dangerous assumption, as year-to-year variation can be substantial. In the case of their work, a *Chlorella vulgaris* culture can produce from 17 to 35 g/m^2/day in summer, depending on the weather of the year. They also considered the biofuel generation process in a more holistic way. Finally, Boruff et al. deployed a similar methodology to evaluate the biofuel production potential of the Western Australian coast [34]. They further refined their methodology by precisely identifying suitable locations through the incorporation of social (workforce availability and education level) and cultural (natives' lands, ecological reserves) elements. All in all, these studies converge on the crucial need to account for local specificities (weather, land suitability and availability, etc.) to deliver meaningful predictions.

Inspired by these previous studies, this work intends to develop a methodology for assessing microalgae biofaçade potential on a large scale. As microalgae biofaçade is a hybrid system, its large-scale assessment requires three crucial elements: adequate microalgae growth model, weather data, and host-building data (equivalent of land quality/availability in the aforementioned studies). The first one was the topic of a set of companion articles, which proposed a numerical model coupling the thermal-biological aspects of the system [21,35] and its application to system design [35,36]. The second one is also accessible thanks to the Météo-France open data policy. Indeed, the French weather forecast agency released almost 30 years of historical weather data covering France's mainland territory. The last one is also openly shared by the French government through the building permits database. By coupling these three elements together, it is possible to assess realistically, in a location-specific manner, the production potential of new buildings constructed in France each year. This article will develop the methodology in a stepwise manner. First, the model will be introduced, and then weather and building data will be diagnosed and curated (a common procedure when using this type of database [37]). Then, the three elements are coupled to evaluate three scenarii (conservative, median, and optimistic) before discussing them.

2. System & models

2.1. Considered system

The modules are foreseen as an alternative to conventional double glazing and thus directly integrated into the structure (as opposed to a double-skin façade). Fig. 1 illustrates a schematic overview of a microalgae biofaçade module optimized from a thermal-biological perspective [21,35]. These investigations screened in a systematic manner different aspects of a module design (dimensions - i.e., reservoir thickness of 3, 5, or 8 cm -, single vs. double glazing, use a radiation selective film - i.e., none, greenhouse type or visible only -, etc.). The optimized system revolves around a reservoir containing the microalgae culture (*Chlorella vulgaris*). This reservoir is enclosed by two sheets of PMMA, distant by 5 cm (ensuring a good compromise between biomass production and static load), and features a gas sparging system at its bottom. On the outward, the system features a conventional double-glazing (15 mm air layer) covered with greenhouse radiation selective films. On the one hand, this combination favors visible light selection — powering photosynthesis — while rejecting infrared radiation — increasing system temperature and leading to acute overheating events —. On the other hand, the double glazing reduces heat loss in a soft manner, incidentally increasing the number of hours adequate for microalgae growth. The dimensions of one biofaçade module are 1 meter in width and 4 meters in height (typical office building floor height). Moreover, the modules are integrated into an office building façade at a height that ensures adequate access to sunlight. One should note that microalgae biofaçade modules are not foreseen to cover the whole façade but alternated (one in two) with conventional double-glazing to ensure visual comfort [15].

2.2. Thermal model

The thermal behavior model of the biofaçade is detailed, validated, and thoroughly analyzed in two companion articles [21,22]. In a nutshell, the model calculates the evolution of the microalgae reservoir temperature by summing the contributions of absorbed and emitted convective-radiative heat fluxes. The considered heat fluxes are of two different natures: weather-modulated and non-weather-modulated. Among the first category are the incident direct sunlight, the incident and emitted radiations from and towards the sky, which are modulated mainly by the cloud cover. They are complemented by the incident and

Fig. 1. Left — Schematic representation of possible microalgae biofaçade design (the aspect ratios and compartments thicknesses are illustrative). 1 — Microalgae culture reservoir, 2 — Outward PMMA layer, 3 — Inward PMMA layer, 4 — Gas sparging system, 5 — Vent, 6 — Double glazing, 7 — Radiation-selective film. Right — Drawing of a potential integration into an office building façade.

emitted radiations towards the surroundings (modulated by surrounding environment temperature and a potential Urban Heat Island effect) and the convective–conductive exchange with the outdoor air (modulated by outdoor air temperature, wind velocity, and direction). The second category contains the incident and emitted radiations from and towards the host building indoors, the convective–conductive exchange with the host building air, the heat inflow carried by the gas sparged into the culture, and the heat outflow extracted by the vented gas.

Conductive heat fluxes within the PMMA and stagnant air layers are described using a resistance in series model. Convective exchanges are modeled based on correlations derived from experimental data. Additionally, solar illumination is described using the model proposed by the Illuminating Engineering Society, which considers solar time, position on Earth, cloud cover, and orientation [38]. Radiative exchanges with the surroundings, given limited information, are modeled using the Stefan–Boltzmann formula weighted by relevant view factors and emissivities. In addition, the spectral component of the different radiative flux is accounted for. To do so, four broad spectral bands were considered: UltraViolet, Visible (subdivided into red, green, and blue), Near InfraRed, and Medium and Far (a.k.a. longwave) InfraRed taken together. All the abovementioned thermal phenomena are described in details in [21] and summarized in the Supplementary Materials.

2.3. Actinic illumination model

Sun and sky actinic illumination are obtained from the model proposed by the Illuminating Engineering Society [38] by restricting it to the photosynthetically active radiation part of the spectrum. Considerations on the absorption of light by the cultures allow to compute two key elements: the light energy absorbed by the culture, which drives cell proliferation, and the averaged level of illumination, which drives cell pigment content and photoconversion efficiency [35]. Further refinement is added by dividing the visible spectrum into three bands: blue, green, and red. For each of them, microalgae exhibit different optical properties, based on the literature [39,40].

2.4. Biological model

The biological model used in this work is based on mass and energy balances [35]. First, cells capture actinic light (based on the illumination calculation and weather modulation). Their ability to harvest and photosynthetic efficiency (fraction of visible light powering photosynthesis, the remainder being turned as heat) are influenced by temperature and the volume-averaged light intensity within the culture compartment (from a practical standpoint, photoinhibition levels are never encountered). Then, the captured energy is used to compute cell proliferation (cells are assumed to have a given Higher Heating Value, allowing the energy to biomass conversion, assuming all other substrates are supplied in excess). In addition to grow, the cells acclimate to the illumination conditions by manipulating their pigment content (increase under low light and the opposite under high illumination). The modulation of light absorption by the cell pigment content is also described by assuming that the absorption cross section is the product of cell pigment content and pigment intrinsic light absorption capacity [39,40]. Furthermore, cell maintenance rate is also differentiated between the day (light respiration) and night (dark respiration) [31], even though it was shown to only have a minor influence on the predictions in the companion article [35]. Finally, cell metabolism as a whole (proliferation, maintenance, and pigment expression) is modulated by temperature [41] (subzero temperatures are never encountered). The cold temperatures slow down cell metabolism but do not damage the cells. On the contrary, the hot temperatures lead to a less efficient metabolism and can even harm the cells if excessive (irreversible denaturation of proteins and DNA [42]). All the abovementioned biological phenomena are described in detail in [35] and summarized in the Supplementary Materials.

2.5. Module control strategy

The biofaçade modules are operated in turbidostat mode by regulating the fraction of incident exiting the culture compartment to 1% of the incident illumination. This value is thought to be a good compromise between maximizing light absorption, hence biomass production, and preserving visual comfort. Indeed, on sunny days, a light of 1% ensures adequate illumination within the workspace (4.61 μmolPhoton/m^2/s, as advised by the US Occupational Safety and Health Administration [43]). Whenever the transmitted light fraction falls below the targeted value, a dilution is ordered. A dilution adds 5% of the culture reservoir as a cell-free fresh medium and withdraws the same volume of cell suspension. In case of hot event, an emergency procedure is implemented. If the reservoir temperature approaches to a temperature lethal for the cells (45.6 °C for *Chlorella vulgaris*), a 95 %-dilution is ordered to make the reservoir translucent and limit power absorption. The safety margin was chosen as the lethal temperature minus twice the standard deviation of the maximum temperature distribution over the hottest year to date (2023, yielding a safety margin of twice 2.69 °C).

3. Data & curation

As described above, a microalgae biofaçade is a hybrid production system at the interface between a building and the outdoor environment. Consequently, it is subjected to weather conditions such

as changes in air temperature, cloud cover, and wind velocity. The variation of the boundary conditions of the system can be described in two ways. First, the problem could be circumvented by using Typical Meteorological Year, a tool generating weather-realistic meteorological data based on the location [44]. However, some limitations exist. For example, the generated data might be somewhat inaccurate in coastal areas or when available meteorological stations are far away from the location of interest. Second, actual weather data can be obtained from a meteorological agency. This last option was chosen for this work. Nevertheless, it also faces some limitations, such as missing data points.

In addition to weather data, building construction data are also solicited in this work. Indeed, biofaçade modules require a host building. Assessing the technology's potential requires estimating the number of new buildings able to host microalgae biofaçade modules. This work used the French building permits database to compute these data.

3.1. Meteorological data

3.1.1. Presentation

Meteorological data driving the model were sourced from Météo-France, the public French weather forecast agency. They cover France with approximately one station per former administrative region (42 stations in total), meshing uniformly the country. The measured data varied from one station to the other as they are not all equipped with the same sensor array. Among the available measurements, the ones used in this study are station ID (to recover name, longitude, and latitude), measurement time, air temperature, cloud cover, wind velocity (at 10 m above the ground), wind direction, relative humidity, dew point, and static pressure (at the station and its variation over 3 h), horizontal visibility, rainfall over the last six hours (only available after 2005), barometric trend, and weather indicator. The ones directly involved in the computation of a microalgae biofaçade module performance are air temperature, cloud cover, wind velocity and direction, relative humidity (for Urban Heat Island Intensity calculation), and static pressure. The others are used to drive the missing value imputation procedure. Feature inclusion was based on inter-station reporting frequency (*i.e.*, found in all stations) and completeness (intra-station data quality). Finally, data range from January 1996 to May 2024 (last access), with measurements taken every three hours, yielding about 62 million data points, of which 12.99% are missing.

3.1.2. Diagnosis

The first step was to check the data for completeness. Fig. 2 reports, per station and per year, the Nan (Not a number) fraction over the whole dataset (Top) and the one specific to the cloud cover (Bottom). The first comment is that overall data quality is variable between stations and over time for each station (Fig. 2 - Top). The main temporal pattern is a higher Nan fraction before 2005, explained by the fact that the rainfall over the last six hours was not reported before this date. Between stations, airport-associated stations are more reliable than the average (ID 7149 — Paris —, ID 7299 — Bale Mulhouse —, 7481 — Lyon, and 7650 — Marseille —). Nevertheless, not all the data have the same role within the model. For example, temperature and cloud cover are paramount. Static pressure is almost accessory as it is used to compute the sparged gas density and associated heat flux, which has been shown to have almost no impact on the system thermal behavior [22].

The first critical parameter is the outdoor air temperature, which strongly influences the culture reservoir temperature, which, in turn, acts on cell metabolic rates. These data were found to be quite robust, with a minimal number of Nan values. Indeed, the yearly fraction of Nan values is 0.10 ± 0.55% - max 13.37% - by station, over 27 years, after the removal of the outlier (ID 7661 — Cap Cepet — on the year 2020 to 2023). Given the marginal amount of Nan values, the missing values were reconstructed by linear interpolation, and the dataset was deemed robust.

The second critical parameter is the cloud cover. Unfortunately, data were more fragmented than for the outdoor air (Fig. 2 - bottom). The first comment is that data availability drops from 2015 onward. This portion of the data might, therefore, not be usable. Over the whole dataset, on average, the yearly amount of Nan values represented 32.08 ± 26.64% by station over 27 years, with some stations (ID 7005, 7255, 7558, and 7577) reporting no value at all for several years in a row (ID 7591 does report cloud cover at all). For the sake of completeness, the dataset was restricted to daytime (9 am to 5 pm), *i.e.*, when cloud cover actually alters sunlight. With this restriction, the average Nan value drops to 21.84 ± 27.31%, indicating that the could cover data are not specifically impacted by the measurement time (*e.g.*, technical problem to measure could coverage at night). If one restricts the dataset to its higher quality part (taking only the data after 2005 and before 2015), these metrics are reduced to 27.59 ± 23.81% (whole day) and 13.84 ± 21.79% (daytime only), which still represents a sizable part of the dataset. The uncertainty surrounding these data is all the more unfortunate as cloud cover has been shown to be a strong modulator of the available light resource driving cell growth. It was, therefore, mandatory to develop a strategy to cope with this partial lack of high-quality data.

3.1.3. Missing value imputation

Two broad categories of approaches are available to reconstruct missing values: statistical methods, and machine learning methods [45]. Among the first ones, imputing the average value or the closest mode value are common practices. Yet, they seem inadequate in the case at hand, as cloud formation is not a random process and could be linked to other available features, opening the way to a rule-based reconstruction. Unfortunately, the covariance matrix does not show a strong correlation between the data. The cloud cover correlation coefficients span from −0.27 to +0.32. Therefore, it was decided to explore machine learning techniques to reconstruct cloud cover data. Cloud cover is either expressed in octa or percent, but, in any case, it is a variable with nine possible values (*e.g.*, 0 to 8). Consequently, a classification approach was adopted over a regression approach. Several algorithms were screened. The output metrics were the Mean Square Error (MSE — the lower, the better), the zero-centeredness of the error ($\bar{e}$ - should be close to zero), the spread of the error (σ_e - the lower, the better), and the accuracy (defined as the percentage of accurate classification). Several classifiers were tested (Support Vector, MultiLayer Perceptron — three layers with 75, 50, 25 REctified Linear Units neurons —, Naive Bayes, K-Nearest Neighbors, Decision Tree, and Random Forest — with 25 trees —). The input features were all the aforementioned ones (excluding station ID but including measurement year to account for slow underlying trends, such as climate change). Performances were screened in cross-validation (10 fold) over a test case (Orly airport station, data from 2005 to date, yielding 53 338 usable data points). The algorithms implementations were drawn from Scikit-learn library [46] and manually tuned before being compared.

Table 1 presents the performances of the different classifiers on the test case. As one can see, Random Forest and MultiLayer Perceptron yield the best results. Random Forest offers zero-centered predictions ($\bar{e}$ close to zero) with lower MSE, and error spread than the MultiLayer Perceptron. Still, the MultiLayer Perceptron achieves the highest accuracy, at the price of being slightly more off-centered. Yet, this better performance cannot be deemed statistically significant. Consequently, Random Forest was used as missing value imputation algorithm.

To reconstruct the cloud cover data, the Random Forest classifier was trained using historical data (after 2005, as rainfall values were not available before this date) specific to each station. This way, data missing on the 2005–2014 period were recreated, accounting for each station specific conditions. Nevertheless, despite missing values reconstruction, some stations had to be discarded because of the irrecoverably poor quality of their data. Namely, station ID 7072 as it had years of missing data, station ID 7181 as it had almost no period where all data were present, and station ID 7591 as it had no cloud cover data.

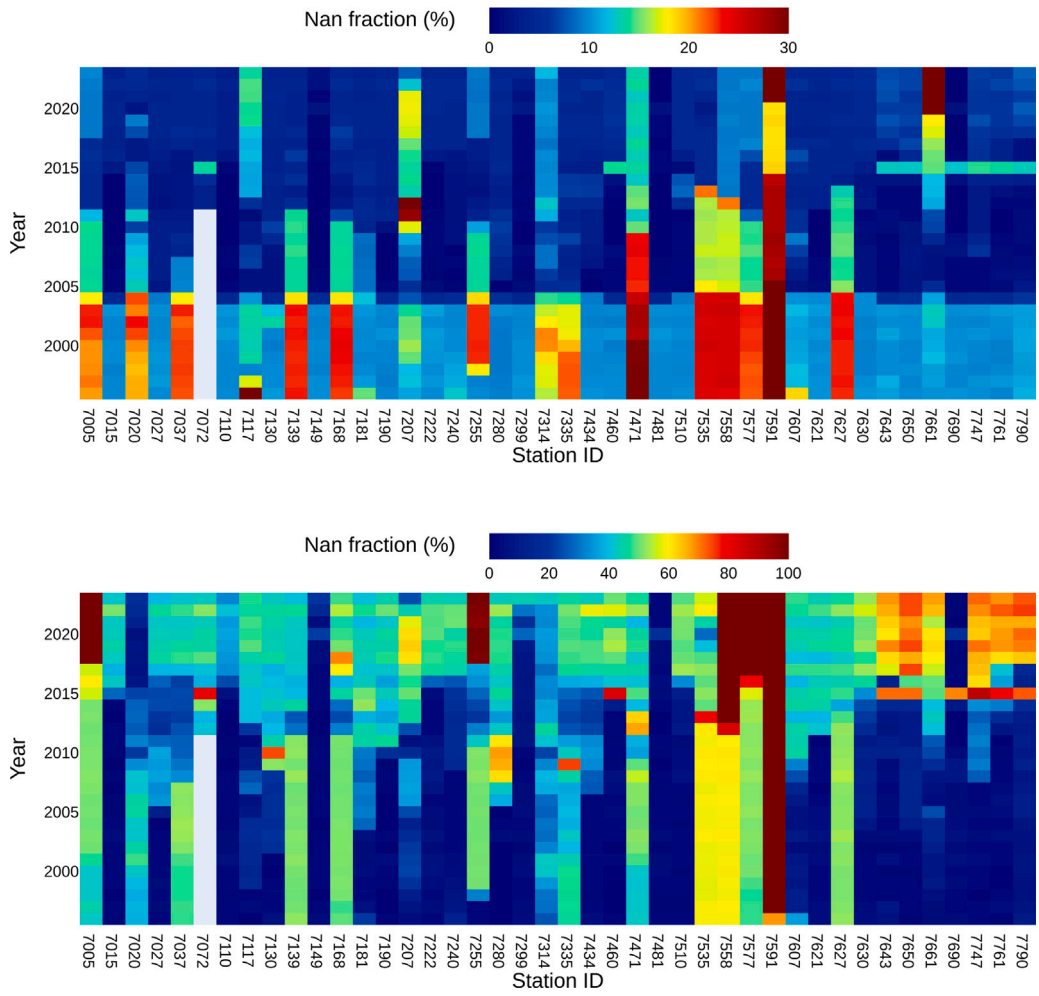

Fig. 2. Top — Nan fraction over the whole dataset. Bottom — Nan fraction for the cloud cover feature. Gray — Missing all data (ID 7072 before 2012).

Table 1
Comparison of the different classification algorithms used to reconstruct cloud cover data. KNN — K-Nearest Neighbors. Bold — Best value. Underlined — Second best value.

Classifier	MSE	$\bar{e}$	σ_e	Accuracy (%)
Support Vector	8.708 ± 0.190	0.810 ± 0.042	2.837 ± 0.029	42.750 ± 0.638
MultiLayer Perceptron	7.626 ± 0.278	0.439 ± 0.142	2.723 ± 0.055	**43.693 ± 0.923**
Naive Bayes	21.077 ± 0.282	−3.289 ± 0.038	3.203 ± 0.019	23.399 ± 0.623
KNN	8.253 ± 0.206	0.077 ± 0.042	2.871 ± 0.036	39.556 ± 0.466
Decision Tree	8.153 ± 0.213	**−0.022 ± 0.047**	2.855 ± 0.037	32.370 ± 0.766
Random Forest	**6.811 ± 0.085**	0.269 ± 0.035	**2.596 ± 0.015**	43.301 ± 0.505

3.1.4. Quality check & interpolation

Once missing data have been corrected, the next step was to check the dataset for the intended application, *i.e.*, computing microalgae biofaçade module performances. The yearly performances of standard modules oriented due South were computed using the model presented above (Section 2). Fig. 3 — Left — presents the annual biomass production of modules, hypothetically placed at the meteorological station locations. As one can see, the performances exhibit a slightly downward trend (−0.12 ± 0.05 kg/year^2, trend over all stations). This trend can be explained by decreasing incident light over the years, driven by an increasing average cloud cover (+1.50 ± 0.41%/year, trend over all stations). In addition, two groups of time series can be identified. The first one shows slightly decreasing performances (Fig. 3 — Right — Green), and the second one exhibits a two-stage downward trend (Fig. 3 — Right — Red). While the initial stage follows the overall trend, the second shows an abrupt (circa −2 kg per year) downshift. The second group of trajectories is the remanence of poor quality of the cloud cover data that the reconstruction could not mitigate. Furthermore, their noise level makes them unreliable and worth removing from the dataset. Hence, it was decided to discard them. To do so, they were identified using a trend criterion (regression coefficient below the average minus one standard deviation) and a noise level criterion with respect to their own trend (Root Mean Square Error > 0.5 kg/year, circa 10% of the annual production). Overall, 27 stations covering relatively uniformly mainland France territory were finally retained for this study.

Once data quality has been ensured, the next step is to interpolate the data between the different locations. Indeed, most of the newly constructed buildings are not located in the vicinity of a meteorological station. After a benchmark, the Adaptive Inverse Weighting Distance algorithm was chosen among the different interpolation techniques, allowing spatial interpolation of a dataset. This technique has been shown to be relevant for large-scale interpolation and is easy to deploy [47]. The choice of the meta parameter (α) governing the spatial

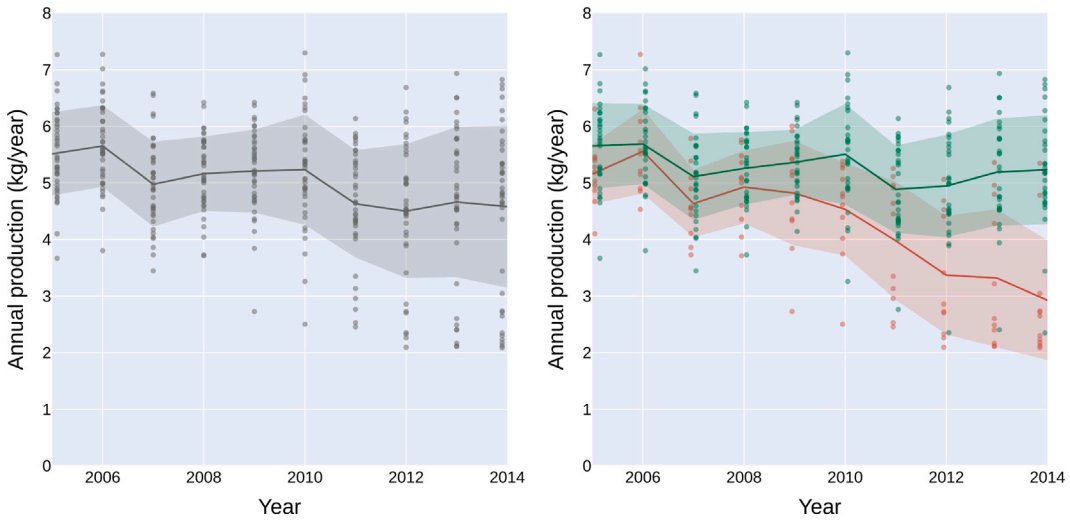

Fig. 3. Annual biomass production for one microalgae biofaçade module placed at the station location. Left — whole dataset. Right — Green — Selected stations. Right — Red — Discarded stations.

decrease of the station influence was obtained by optimization and ten-fold cross-validation using the data of the first year of the selected dataset. The calibrated interpolation obtained an RMSE of 0.62 kg for an average production of 5.73 kg per biofaçade module, yielding a 10.8% error, which was deemed acceptable for the interpolation. This way, a mapping of the annual production per module could be computed over the whole country. Thus, each new building could see its microalgae production potential evaluated based on its geographical coordinates (see Graphical Abstract).

3.2. Building permits data

3.2.1. Presentation

Microalgae biofaçade being a hybrid building/biotechnology system, it is important to identify candidate host buildings to assess the production potential over France. Thanks to the French government's open data policy, building permits data is publicly available today. This database contains records since 2013, with 690657 entries for nonresidential buildings over the 2013–2023 period. Each entry has 99 features, most of them being zero-filled as not all features relevantly apply to each entry. Among the available data, the ones of interest for this work are the municipality code of the building (to identify its longitude and latitude and the urban density of the associated area), intended use (housing, hotel, office, retail, craftsmanship, industry, agriculture, warehouse, administrative), project status (authorized, canceled, started, completed), type of the project (new building or renovation), effective starting date, project lot area, project total area, and number of floors of the building (introduced in 2020, deemed poorly reliable in the metadata). The two last features were combined to yield the area per floor (project total area/nb. of floors) and the façade length (square root of the floor area, assuming a square shape).

In addition to the building permits database, the INSEE (French Institute of Statistics and Economic Studies) database detailing the urban density for each municipality was accessed to assess the surrounding of biofaçade installations (*e.g.*, city center with tall buildings, rural area with open access to the sunlight, etc.). These data are based on a 1 km^2 square meshing of France's mainland territory done by Eurostat (the statistical office of the European Union) retreated by INSEE in 2022 based on the 2018 population survey. Following a specific methodology to identify urban centers, INSEE classified the municipalities as very low (< 25 inhab./km^2), low (< 300 inhab./km^2), medium (< 1500 inhab./km^2), and high (> 1500 inhab./km^2) density area. This methodology clearly ensures a high quality of the data, as, in France, some municipalities span vast areas, which could induce erroneous classification if the overall population density (number of inhabitants/municipality area) was used instead.

3.2.2. Diagnosis

The first comment is that the building permits databases had extremely few empty cells over the features of interest (4656 over 18969741, *i.e.*, 0.02%). The second database, detailing the urban density, was also complete. Furthermore, Nan values could not be used as indicators as some values are text, hence, naturally not numbers. Nevertheless, data quality could be diagnosed based on a set of criteria identifying erroneous data provision (*i.e.*, leading to abnormal buildings). Those criteria were: more than 50 floors for a building, one-floor area larger than the lot area, one-floor area below 1 m^2, and incorrect municipality code (not provided, Nan, not in found in the official municipality database). On average, per year, 7.96 ± 0.48% of the records were erroneous for the period spanning from 2013 to 2023 (Table 2). Data can, therefore, be deemed of good technical quality. Yet, two additional comments are to be drawn.

First, the keen observer would have noted that the number of canceled projects is relatively stable over the year 2015 to 2020 (3.59 ± 0.17%) and drops over the year 2021 to 2023. This is explained by the fact that a project cancellation may be issued several years after its authorization (up to three years, based on the data). Therefore, to avoid overestimating the number of new buildings over the year 2021, 2022, and 2023, the lower cancellation rating over the most recent period had to be corrected. The first step is to analyze if canceled projects exhibit a specific pattern with respect to the whole data. To do so, the relative distance between the canceled projects subset and the rest of the dataset was measured. As measuring a distance in the features space is not intuitive, a specific metric was used: Cohen'd (Eq. (1), [48,49]). This index compares the distance between two groups by weighting it with the joint standard deviation, which eases the comparison. In terms of interpretation, an absolute Cohen's d value of 0.2 is deemed minor, 0.5 medium, and large above 0.8. Over the different building categories, Cohen'd values reach an average of 0.06 ± 0.03 - max 0.11 -. Consequently, it can be concluded that the canceled projects are not significantly different from the whole dataset. Therefore, it is possible to correct the cancellation level over 2021–2023 by artificiality marking randomly some projects as canceled until the cancellation rate reaches the one on the 2015–2020 period.

$$d = \frac{\bar{X}_1 - \bar{X}_2}{\sqrt{\frac{s_1^2 + s_2^2}{2}}} \tag{1}$$

The second comment to be drawn is that the database manager specifies in the metadata that some data, were unreliable, among which the number of floors. Unfortunately, this information is paramount for

Table 2
Data curation and selection from the building permits database.

Year	Number of records							Relative values			
	Nb. of projects	Nb. floors >50	Larger than the lot	Below 1m^2 per floor	No municipality code	Unknown municipality code	Canceled	Selected	Incorrect	Canceled	Selected
2013	79 304	2	2993	22	546	2991	3742	40 342	8.26%	4.72%	50.87%
2014	68 013	3	2899	12	1242	722	3299	34 609	7.17%	4.85%	50.89%
2015	65 870	5	2841	24	1372	785	2417	33 333	7.63%	3.67%	50.60%
2016	68 805	1	3126	29	1662	864	2293	35 194	8.26%	3.33%	51.15%
2017	62 884	4	3303	25	1444	707	2232	30 846	8.72%	3.55%	49.05%
2018	59 498	5	3084	39	1302	602	2071	28 130	8.46%	3.48%	47.28%
2019	59 756	3	3257	35	1166	529	2281	27 983	8.35%	3.82%	46.83%
2020	51 079	1	2674	21	993	342	1881	23 951	7.89%	3.68%	46.89%
2021	61 500	10	3243	33	1185	311	1957	31 474	7.78%	3.18%	51.18%
2022	59 712	5	3233	38	829	320	1526	31 049	7.41%	2.56%	52.00%
2023	54 236	8	2669	58	302	1123	493	29 663	7.67%	0.91%	54.69%

this work, which enforces the need for additional curation to ensure the reliability of the data.

3.2.3. Curation

To minimize the curation workload, as the deployed algorithms could be computational power greedy, this curation was carried out on data that were relevant for the study. Data were retained based on the type of the project (new constructions, renovations were excluded), project status (canceled projects were excluded), and floor area (minimum 25 m^2 for one floor). These selection criteria resulted in the inclusion of 50.13 ± 2.42% of the records per year over the 2013–2023 period. Then, data were further restricted to those filed after 2020, as the number of floors was not requested to file for a building permit before this date. Hence, floor area and façade length cannot be established for records before this date. This narrowed the usable data to 92186 records on which further curation was undergone.

Subsequent data curation was led in two stages. First, outliers were detected and removed using DBSCAN unsupervised clustering algorithm [50] based on façade length and number of floors (after data scaling). Then, cluster analysis was performed to identify those associated with erroneous data provision. Problematic clusters were defined as those featuring buildings having abnormal characteristics (too many floors for a too-small façade), *i.e.*, two-floor buildings with a side length below 10 m or three-floor buildings with a side length below 15 m. This procedure was carried out individually on subsets grouping records per intended final use (office, retail, industry, etc.). For each of them, DBSCAN meta-parameters (search distance and minimum number of members to create a cluster) were jointly optimized to avoid classifying all records as outliers or as members of the same supercluster. Fig. 4 shows the results of the outliers (black dots) detection and abnormal building (red dots) identification procedures for the office buildings subset. Even though visually important, outliers only represent 9.8% of the 5267 records. While they might appear as possible buildings layout at first, one has to think of how likely would be the average outlier: a single-story building with 100 m of façacade length (*i.e.*, 10 000 m^2 of area). In addition, the clusters hosting buildings with questionable façade length to floor number ratio encompasses 18.1% of the data. They are thought to originate from erroneous provision of the building number of floor.

By repeating this process for all the type of building, the final dataset contained 48742 records, over the year 2021 to 2023, deemed trustworthy enough to be used in the rest of the workflow.

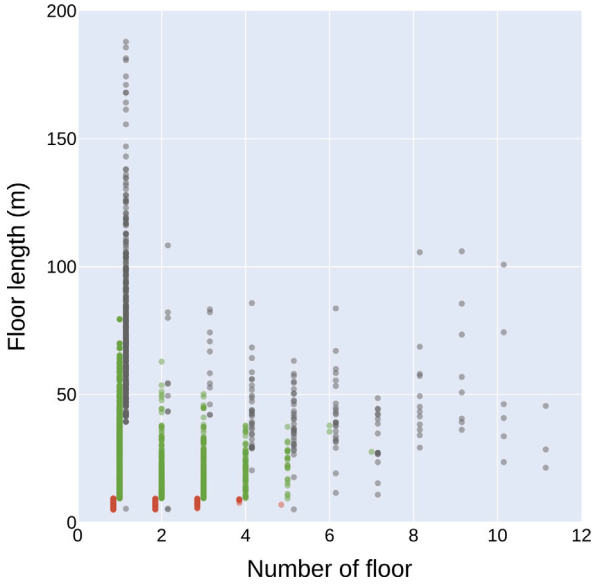

Fig. 4. Clustering curation procedure results for the office buildings subset. Green — Selected entries. Red — Discarded entries (abnormal characteristics clusters). Black — Outliers.

4. Scenarii

After reconstructing weather data, broadcasting microalgae biofaçade module production over the whole territory, and locating new buildings implementations, the next step was to couple them together. This can be done straightforwardly using the buildings municipality codes to recover their geographical coordinates. The last point was to assess the buildings' surroundings as they can modulate the biofaçade module's thermal behavior depending on whether they induce an Urban Heat Island phenomenon. This work considered that the Urban Heat Island phenomenon comes into play for medium and high-density municipalities (identified thanks to INSEE database).

Once technical details have been sorted out, the deployment scenarii can be designed. A scenario is a set of specific conditions for a deployment to be considered relevant. It specifies which building types can host a microalgae biofaçade, the associated load (fraction of a façade covered by microalgae culture modules), minimal height (in number of floors) to ensure adequate access to sunlight, the minimal production a module has to achieve, and the minimal production a building has to achieve to be included. Table 3 details the three scenarii considered in this work. As one can see, no warehouses or agricultural buildings are included as potential targets as they are not equipped with heating systems, which dramatically hinders the synergy between building and the microalgae culture. In addition, housings are also excluded as managing the workflow associated with culture medium sourcing and biomass valorization was deemed too troublesome for the general public. Furthermore, in all the scenarii, the building load does not exceed 50% of the façade, as it was shown to be the maximum value still ensuring adequate visual comfort [15]. In addition, the

Table 3
Scenarii characteristics.

Scenario	Building type	Façade load	Minimum module height	Minimum production per module (kg/year)	Minimum production per building (kg/year)
Optimistic	Office	50%	Very low density — Ground floor	1.67	25
	Retail	50%	Low density — Ground floor		
	Industry	33%	Medium density — Second floor		
	Hotel	50%	High density — Third floor		
	State/Administrative	50%			
Median	Office	50%	Very low density — Ground floor	2.5	50
	Retail	50%	Low density — Ground floor		
	Industry	25%	Medium density — Second floor		
	Hotel	50%	High density — Fourth floor		
	State/Administrative	50%			
Conservative	Office	50%	Very low density – Ground floor	3.33	75
	Retail	50%	Low density — Ground floor		
	Industry	10%	Medium density — Third floor		
	Hotel	50%	High density — Fifth floor		
	State/Administrative	50%			

industry buildings load was set to lower values. Indeed, most industrial installation include buildings that are not heated (storage, expedition hall, etc.). For the tested scenarii, the outcomes are the microalgae production potential offered by newly constructed buildings over a given year and the number of microalgae biofaçade module to be produced to equip the new buildings (to evaluate the need for a specific industry).

Three scenarii were designed assuming different set of hypotheses. The optimistic scenario assumes that most of the buildings could host microalgae biofaçade modules with a load of 33% for industrial façades. In addition, it assumes that in the cities (medium and high-density municipalities), the lower floors of the buildings have adequate access to sunlight. Finally, it accepts lower productivity modules (1.67 kg/year, 33% of the reference value of 5.06 kg/year, the average for South-oriented modules) and buildings (25 kg/year). The median scenario is more exigent as higher elevation is required in cities to access sunlight, and only modules yielding at least 50% of the reference capacity are included. The conservative scenario can be deemed stringent as high elevation is required in cities, and only the most efficient modules are selected if the overall building production potential is high (more than 75 kg/year).

Finally, the scenarii simulation requires addressing the mismatch between the available data and some adjustments to account for uncertainties originating from unknown buildings' orientations. Quality weather data span from 2005 to 2014, while the usable records section of the building permits database (with the number of floors of the construction) covers the years 2021, 2022, and 2023. Therefore, the production capacities of the new buildings were evaluated using weather records from about ten years ago obtained at the same location. While not optimal, this methodology was chosen as data quality was preferred over data concomitance. Furthermore, the building average lifespan is of several decades, which minimizes the importance of the time difference between the two datasets. Regarding building orientation, it would be bold to assume that all the façades are oriented towards the South. Indeed, orientation is more likely to be dictated by the lot shape than the will to cultivate microalgae. Therefore, façade orientation was assumed random between all the possible directions, with a 22.5 ° increment. When two façades are exposed to the South (*e.g.*, the South-East is complemented by the South-West), both are tested to determine whether they could host a valid implementation. As the orientation affectation procedure is random, it requires to be repeated several times to avoid unintentionally selecting an artifact. Consequently, it was carried out until the convergence of the performance indicators' average and standard deviation (40 Monte Carlo runs were enough to achieve a convergence below 5%).

5. Prediction analysis

Fig. 5 illustrates the proposed methodology outputs at the country scale. As one can see on the left side of the figure, microalgae biofaçade modules are more productive in the coastal areas next to the Atlantic Ocean and the Mediterranean Sea, with productions of up to 8 kg per year for a South-oriented module. On the contrary, the inland eastern part of mainland France is less favorable, with locations allowing an output below 4 kg per year. In addition, the map also delivers insights into new office building locations in the year 2021. They are preferentially located in the western part of the country, with hot spots in metropolises. Regarding yearly generated production potential agglomerated at the nation scale, it ranges from +28.9 ± 3.7 ton per year to +202.6 ± 17.4 ton per year, depending on the scenario. In the case of the optimistic and the median scenario, all the building categories contribute to biomass production, with significant contributions from the largest buildings (state and retail). Yet, the extent of their contribution is halved between the two sets of rules. Going one step further, the conservative scenario excludes hotel and industry buildings but retains retail ones, which become the dominant type. From this analysis, it can be concluded that, in France, the surest growth vector for microalgae biofaçade are the retail buildings (*e.g.*, malls), followed by state buildings, and, finally, office buildings. Finally, in any of the scenarii, the number of required microalgae biofaçade modules is more than enough to sustain year-round continuous production (from 6100 to 62,000 units), making them an economically attractive product for a window manufacturer.

Having access to a sizable amount of data allows to dive into the details and investigate performance distributions in addition to agglomerated indicators. Fig. 6 presents the distribution of the new office building production distribution potential, the number of modules per building, and the specific production for each module. The first comment is that the distribution of the indicators is remarkably stable over the three tested years. Furthermore, the building production potential and the number of installed modules per building exhibit a log-normal distribution of almost constant mean and standard deviation (Table 4). While it is exemplified for the office buildings, the same comment can be drawn for the other types of buildings. The last indicator (individual module annual production) does not follow the same trend as the two first ones. This distribution is made of several Gaussian components. Each component corresponds to an orientation (South, South-South-East, South-East, etc. and their West counterparts). It is specifically interesting to note that the South-facing modules exhibit far better performance than the others. This highlights the fact that orientation determines the system performance (mean of the individual Gaussian curves), while location only modulates it (standard deviation of the Gaussian curves). From this analysis of these distributions, it can be

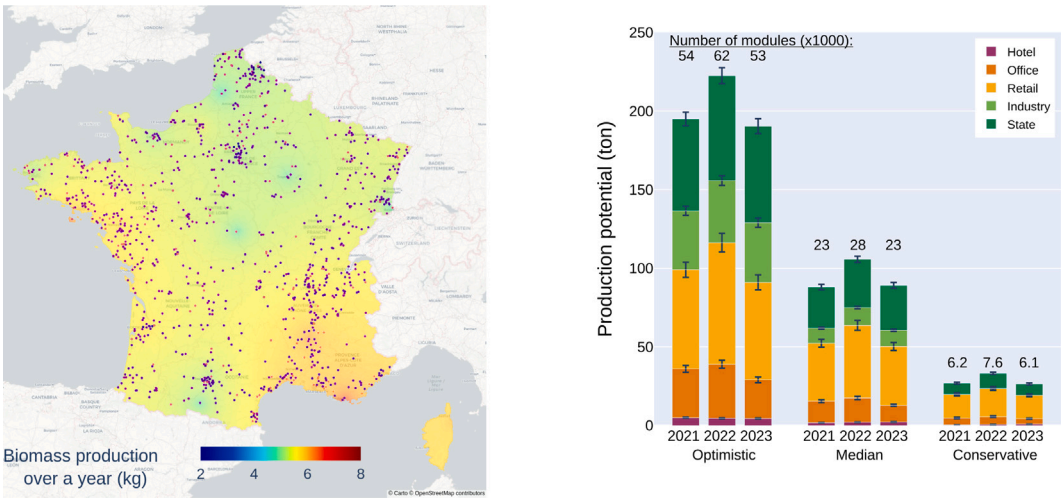

Fig. 5. Left — Projection of the map of the new office buildings for year 2021. Color scale — Performance of one module, randomly oriented. Right — France-scale production for the different scenarii.

Table 4
Parameters resulting the distributions fitting. Values are displayed as average ± standard deviation over the year 2021, 2022, and 2023.

	Production potential		Number of module per building		Individual module production (two first Gaussian curves out of three)			
	Mean (kg/year)	Std. Dev. (kg/year)	Mean (–)	Std. Dev. (–)	Mean (kg/year)	Std. Dev. (kg/year)	Mean (kg/year)	Std. Dev. (kg/year)
Office	72.0 ± 3.1	36.5 ± 1.1	19.9 ± 0.7	9.7 ± 0.3	5.36 ± 0.01	0.36 ± 0.01	3.36 ± 0.05	0.65 ± 0.01
Retail	94.9 ± 0.4	50.6 ± 0.2	26.2 ± 0.2	13.6 ± 0.1	5.36 ± 0.01	0.31 ± 0.00	3.39 ± 0.00	0.58 ± 0.01
Industry	76.3 ± 2.2	65.4 ± 3.0	21.0 ± 0.6	17.6 ± 0.7	5.37 ± 0.00	0.32 ± 0.01	3.39 ± 0.01	0.54 ± 0.01
Hotel	52.0 ± 3.5	36.4 ± 3.3	14.4 ± 1.0	10.0 ± 1.1	5.34 ± 0.05	0.30 ± 0.07	3.38 ± 0.07	0.53 ± 0.08
State	71.0 ± 4.9	36.7 ± 1.8	20.7 ± 0.1	10.4 ± 0.1	5.34 ± 0.01	0.34 ± 0.01	3.34 ± 0.02	0.58 ± 0.01

concluded that few buildings have a high production potential and that orientation is the first factor governing system performance.

6. Discussion

The estimations drawn by the proposed methodology call for a discussion. First, the cloud cover data are to be confronted with other available data. This is especially true for the trend. Indeed, specific values may have been reconstructed, but the available data give the trend itself. The overall trend over the 2005–2014 period is an increase at a rate of +1.00 ± 0.30%/year for the selected stations. This value might seem small, yet it represents an increase of 10% over ten years, which is subsequent. As a point of comparison, over mainland USA, the increase rate was +0.19 to +0.27%/year over the preceding 34 years, according to Dai et al. [51]. Interestingly, the authors noted that cloud cover monitoring was a complex task for which different observation techniques (human observation, ground-level monitoring — ceilometer -, and satellite monitoring) yield different values. They also advocated that ceilometers yield measurements of lower quality than human observers. This difference was also acknowledged by Météo-France, yet the cost reduction it offers led to a large deployment of the technology. Indeed, at the end of 2005, all French large airports were equipped with this technology [52]. Therefore, it is safe to assume that all stations were also equipped, as airports are tied to strong regulations that prevent the rapid replacement of humans by machines. Furthermore cloud cover correlation with rainfall was also lower in this study (+0.12) than the one reported by Dai et al. (+0.35) [51], which may indicate that France would be covered by more clouds less prone to rain. In addition to comparing the literature, contacting Météo-France to gather their expert opinions was unsuccessful. Nevertheless, none of these elements would void the validity of the methodology used in this work.

Building data is also to be confronted with literature. While it is difficult to find academic work directly relating to the data at hand, it is possible to note that most of the buildings found in the database have five floors or less (Fig. 4). This observation echoes the one of Godoy-Shimizu et al. who concluded that low-rise buildings (*i.e.*, less than five floors) are more efficient energetically efficient than their higher-rise counterparts [37]. In addition to their distribution, the lifespan of buildings is also a key parameter to be considered, as it dictates how long the deployed system can be used. The explored building types belong to the "common building" and should be designed to last 50 years, according to European guidelines [53]. Nevertheless, studies show that buildings lifespan is longer than the prescription (from 70 to 100 years for ordinary buildings [37,54]). Assuming a conservative 50-year lifespan would allow, once fully deployed, French microalgae biofaçades to produce 1.4 ± 0.2, 4.7 ± 0.5, and 10.1 ± 0.9 kton/year according to the conservative, the median, and the optimistic scenario, respectively.

Finally, evaluating the capacity of the production system is only relevant when compared to the market in addresses. In the case of this work, as microalgae biofaçade modules would be implemented in France and host *Chlorella vulgaris* cultures, the intended market can be described as the European market for this strain. Yet, European microalgae production markets and volumes are difficult to evaluate. On the one hand, microalgae enthusiastic lobbies evaluate the market to be around 25 ktons (all species) per year in 2030, for a market value of half a billion USD. On the other hand, official data from the Food and Agriculture Organization (FAO) [55], acknowledged by the European institutions [56], lie around 250 tons, which is an underevaluation. Indeed, when accessing the FAO data, one finds an almost empty database, dominated by *Arthrospira* production (102 kton in 2022, appearing as 99.68% of the worldwide microalgae production) with almost no mention of the *Chlorella* genus (which is cautiously estimated around 5 kton worldwide per year, based on the author's contacts in the industry). In an in-depth survey, Araujo et al. corroborated this analysis with the statement, "Official statistics on microalgae production volumes are almost non-existent at the European scale, and the data

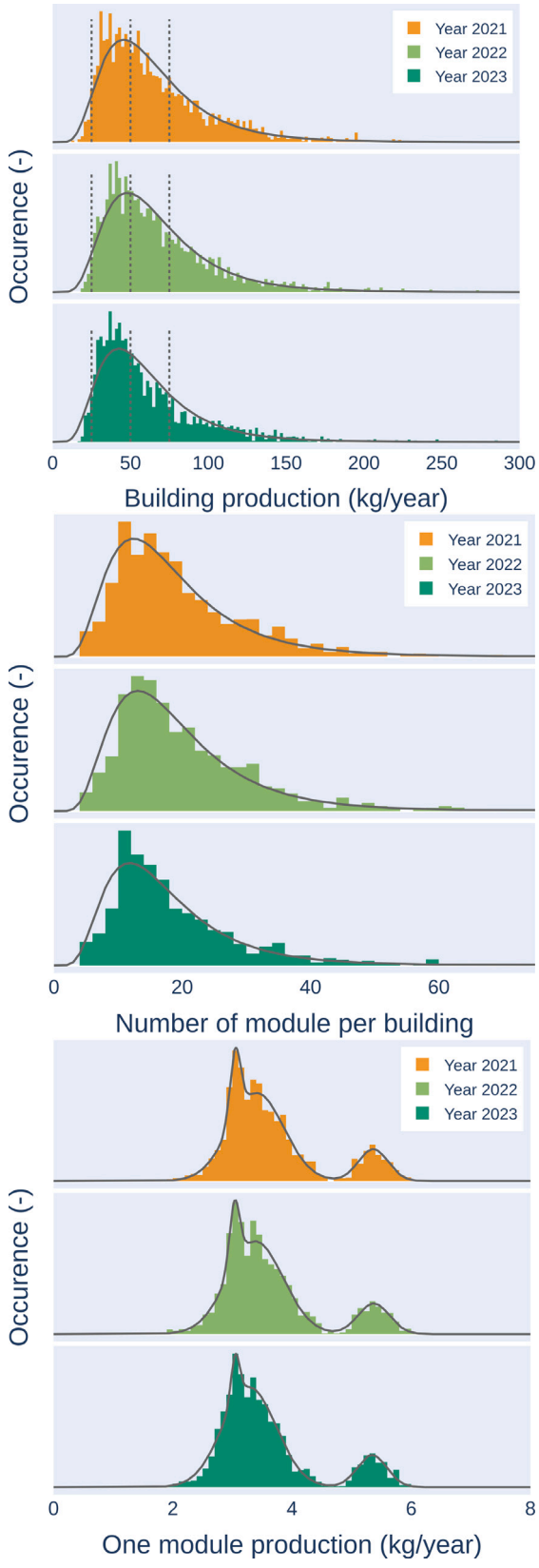

Fig. 6. Top — Building production distribution potential before final selection is applied. Continuous line — Log-normal distribution fit. Dashed line — Scenarii threshold values for single building production. Middle — Distribution of the number of microalgae biofaçade module per building. Continuous line — Log-normal distribution fit. Bottom — Distribution of newly implemented modules annual production. Continuous line — Triple Gaussian fit.

available from FAO or Eurostat are limited and fragmented" [57]. Going further, and working with the European Algae Biomass Association, the authors estimated European production around 80 ton per year for *Chlorella* species, with no estimation of potential importations. In addition to volume, adequacy of the biomass quality (pigment content, protein content, low bacterial contamination [58]) with the market demand would also have to be ensured. Here, the foreseen biomass pigment content could range from 25 to 44 mg/g, which is relatively high ensuring high biomass quality [36]. Thus, all in all, "guestimating" a 10 kton worldwide market volume for *Chlorella* genus, with a third of the consumption in Europe, *i.e.*, 3.3 kton per year, the conservative scenario applied to France is able to cover a sizable fraction (44%) of the European needs.

7. Conclusion

This work combined open big data from the French weather forecast agency and the French government to evaluate the annual deployment potential for microalgae biofaçade over France's mainland territory. Even though data curation was mandatory, three scenarii were evaluated. The annual production potential offered by new buildings lies between +28.9 ± 3.7 and +202.6 ± 17.4 ton per year for the conservative and the optimistic scenario, respectively. It corresponds to producing 6100 to 62,000 microalgae biofaçade units, which is more than enough to sustain year-round continuous production. Analyzing the host building type revealed that retail buildings (*e.g.*, malls) are the most favorable places for the technology, followed by state buildings and offices. Finally, in depth analysis of the results showed that façade orientation is the first predictor of the system performance while its geographical location in France is only a modulator of it.

Declaration of competing interest

The authors declare that they have no known competing financial interests or personal relationships that could have appeared to influence the work reported in this paper.

Acknowledgments

Communauté urbaine du Grand Reims, Département de la Marne, Région Grand Est and European Union (FEDER Grand Est 2021–2027) are acknowledged for their financial support to the Chair of Biotechnology of CentraleSupélec and the Centre Européen de Biotechnologie et de Bioéconomie (CEBB).

Appendix A. Supplementary data

Supplementary material related to this article can be found online at https://doi.org/10.1016/j.renene.2025.123406.

Data availability

Model & Data availability

A Python implementation of the proposed model is freely available at https://github.com/victorpozzobon/biofacade.

Weather data can be recovered from https://www.data.gouv.fr/en/datasets/donnees-d-observation-des-principales-stations-meteorologiques/.

Building permits data be downloaded from https://www.statistiques.developpement-durable.gouv.fr/catalogue?page=dataset&datasetId=6513f0189d7d312c80ec5b5b.

Population density data can be found at https://www.insee.fr/fr/information/2114627.

Zipcode can be linked to geographical coordinates thanks to https://www.data.gouv.fr/fr/datasets/communes-de-france-base-des-codes-postaux/.

References

[1] Global footprint network, 2024.

[2] S. Díaz, J. Settele, E. Brondizio, H.T. Ngo, M. Guèze, J. Agard, C. Zayas, IPBES global assessment: summary for policymakers, 2019, Retrieved from IPBES website, https://www.ipbes.net/news/ipbes-global.

[3] A.K. Koyande, K.W. Chew, K. Rambabu, Y. Tao, D.-T. Chu, P.-L. Show, Microalgae: A potential alternative to health supplementation for humans, Food Sci. Hum. Wellness 8 (1) (2019) 16–24.

[4] M. Rizwan, G. Mujtaba, S.A. Memon, K. Lee, N. Rashid, Exploring the potential of microalgae for new biotechnology applications and beyond: A review, Renew. Sustain. Energy Rev. 92 (2018) 394–404.

[5] W. Levasseur, P. Perrè, V. Pozzobon, A review of high value-added molecules production by microalgae in light of the classification, Biotech. Adv. 41 (2020) 107545.

[6] C. Camarena-Bernard, V. Pozzobon, Evolving perspectives on lutein production from microalgae - a focus on productivity and heterotrophic culture, Biotech. Adv. (2024) 108375.

[7] H.R. Molitor, E.J. Moore, J.L. Schnoor, Maximum CO2 utilization by nutritious microalgae, ACS Sustain. Chem. Eng. 7 (10) (2019) 9474–9479, Publisher: American Chemical Society.

[8] N. Brown, A. Shilton, Luxury uptake of phosphorus by microalgae in waste stabilisation ponds: current understanding and future direction, Rev. Environ. Sci. Bio. Technol. 13 (3) (2014) 321–328.

[9] J.A. Hellebust, I. Ahmad, Regulation of nitrogen assimilation in green microalgae, Biol. Ocean. 6 (3–4) (1989) 241–255, Publisher: Taylor & Francis _eprint: https://www.tandfonline.com/doi/pdf/10.1080/01965581.1988.10749529.

[10] P.K.C. Sasi, J.M. AmbilyViswanathan, D.M. Thomas, J.P. Jacob, S.V. Paulose, Phycoremediation of paper and pulp mill effluent using planktochlorella nurekis and chlamydomonas reinhardtiia comparative study, J. Environ. Treat. Tech. 8 (2) (2020) 809–817.

[11] J. Ruiz, G. Olivieri, J.d. Vree, R. Bosma, P. Willems, J.H. Reith, M.H.M. Eppink, D.M.M. Kleinegris, R.H. Wijffels, M.J. Barbosa, Towards industrial products from microalgae, Energy Environ. Sci. 9 (10) (2016) 3036–3043, Publisher: The Royal Society of Chemistry.

[12] M. Talaei, M. Mahdavinejad, R. Azari, Thermal and energy performance of algae bioreactive façades: A review, J. Build. Eng. 28 (2020) 101011.

[13] R. Mahrous, E. Giancola, A. Osman, T. Asawa, H. Mahmoud, Review of key factors that affect the implementation of bio-receptive façades in a hot arid climate: Case study north Egypt, Build. Environ. 214 (2022) 108920.

[14] R.A. Agathokleous, S.A. Kalogirou, Double skin facades (DSF) and building integrated photovoltaics (bipv): a review of configurations and heat transfer characteristics, Renew. Energy (2016).

[15] H. Sarmadi, M. Mahdavinejad, A designerly approach to Algae-based large open office curtain wall Façades to integrated visual comfort and daylight efficiency, Sol. Energy 251 (2023) 350–365.

[16] H. Rezazadeh, Z. Salahshoor, F. Ahmadi, F. Nasrollahi, Reduction of carbon dioxide by bio-façades for sustainable development of the environment, Environ. Eng. Res. 27 (2) (2022) ISBN: 1226-1025 Publisher: Korean Society of Environmental Engineers.

[17] F. Ahmadi, S. Wilkinson, H. Rezazadeh, S. Keawsawasvong, Q. Najafi, A. Masoumi, Energy efficient glazing: A comparison of microalgae photobioreactor and Iranian Orosi window designs, Build. Environ. 233 (2023) 109942.

[18] E.S. Umdu, I. Kahraman, N. Yildirim, L. Bilir, Optimization of microalgae panel bioreactor thermal transmission property for building façade applications, Energy Build. 175 (2018) 113–120.

[19] J. Pruvost, B. Le Gouic, O. Lepine, J. Legrand, F. Le Borgne, Microalgae culture in building-integrated photobioreactors: Biomass production modelling and energetic analysis, Chem. Eng. J. 284 (2016) 850–861.

[20] C. Barajas Ferreira, L. Castro Padilla, G.V. Sánchez, A.D. González-Delgado, a.F. Barajas Solano, Design of a microalgae bio-reactive facade reactor for cultivation of Chlorella vulgaris, Contemp. Eng. Sci. 10 (22 (2017)) (2017) 1067–1074, Accepted: 2021-12-01T16:34:12Z Publisher: Contemporary Engineering Sciences.

[21] V. Pozzobon, Microalgae bio-reactive façade: A radiative-convective model powered by hourly illumination computation and historical weather data, J. Build. Eng. 90 (2024) 109407.

[22] V. Pozzobon, Microalgae bio-reactive façade: Location and weather-based systematic optimization, Build. Environ. 253 (2024) 111352.

[23] A.M. Elmalky, M.T. Araji, Computational fluid dynamics using finite volume method: A numerical model for double skin façades with renewable energy source in cold climates, J. Build. Eng. 60 (2022) 105231.

[24] A.M. Elmalky, M.T. Araji, Multi-objective problem of optimizing heat transfer and energy production in algal bioreactive façades, Energy 268 (2023) 126650.

[25] A.M. Elmalky, M.T. Araji, Optimization models for photosynthetic bioenergy generation in building façades, Renew. Energy 228 (2024) 120607.

[26] E. Todisco, J. Louveau, C. Thobie, E. Dechandol, L. Hervé, S. Durécu, M. Titica, J. Pruvost, A dynamic model for temperature prediction in a façade-integrated photobioreactor, Chem. Eng. Res. Des. 181 (2022) 371–383.

[27] F. Girard, C. Toublanc, Y. Andres, E. Dechandol, J. Pruvost, System modeling of the thermal behavior of a building equipped with facade-integrated photobioreactors: Validation and comparative analysis, Energy Build. 292 (2023) 113147.

[28] J. Wurm, M. Pauli, SolarLeaf: The world's first bioreactive façade, Arq: Archit. Res. Q. 20 (1) (2016) 73–79, Publisher: Cambridge University Press.

[29] I. Wagner, C. Steinweg, C. Posten, Mono- and dichromatic LED illumination leads to enhanced growth and energy conversion for high-efficiency cultivation of microalgae for application in space, Biotechnol. J. 11 (8) (2016) 1060–1071, _eprint: https://onlinelibrary.wiley.com/doi/pdf/10.1002/biot.201500357.

[30] R. Dillschneider, C. Steinweg, R. Rosello-Sastre, C. Posten, Biofuels from microalgae: Photoconversion efficiency during lipid accumulation, Bioresour. Technol. 142 (2013) 647–654.

[31] A. Oliver, C. Camarena-Bernard, J. Lagirarde, V. Pozzobon, Assessment of photosynthetic carbon capture versus carbon footprint of an industrial microalgal process, Appl. Sci. 13 (8) (2023) 5193, Number: 8 Publisher: Multidisciplinary Digital Publishing Institute.

[32] J.W. Moody, C.M. McGinty, J.C. Quinn, Global evaluation of biofuel potential from microalgae, Proc. Natl. Acad. Sci. 111 (23) (2014) 8691–8696, Publisher: Proceedings of the National Academy of Sciences.

[33] A.M. Coleman, J.M. Abodeely, R.L. Skaggs, W.A. Moeglein, D.T. Newby, E.R. Venteris, M.S. Wigmosta, An integrated assessment of location-dependent scaling for microalgae biofuel production facilities, Algal Res. 5 (2014) 79–94.

[34] B.J. Boruff, N.R. Moheimani, M.A. Borowitzka, Identifying locations for large-scale microalgae cultivation in western Australia: A GIS approach, Appl. Energy 149 (2015) 379–391.

[35] V. Pozzobon, Microalgae bio-reactive façade: A model coupling weather, illumination, temperature, and cell growth over the year, Renew. Energy 237 (2024) 121545.

[36] V. Pozzobon, Microalgae bio-reactive façade: System thermalbiological optimization, Renew. Energy 235 (2024) 121377.

[37] D. Godoy-Shimizu, P. Steadman, I. Hamilton, M. Donn, S. Evans, G. Moreno, H. Shayesteh, Energy use and height in office buildings, Build. Res. Inf. 46 (8) (2018) 845–863, Publisher: Routledge _eprint: https://doi.org/10.1080/09613218.2018.1479927.

[38] Recommended practice for the calculation of daylight availability, J. Illum. Eng. Soc. 13 (4) (1984) 381–392, Publisher: Taylor & Francis _eprint: https://doi.org/10.1080/00994480.1984.10748791.

[39] R. Kandilian, A. Soulies, J. Pruvost, B. Rousseau, J. Legrand, L. Pilon, Simple method for measuring the spectral absorption cross-section of microalgae, Chem. Eng. Sci. 146 (2016) 357–368.

[40] B. Baránková, D. Lazár, J. Nau, A. Solovchenko, O. Gorelova, O. Baulina, G. Huber, L. Nedbal, Light absorption and scattering by high light-tolerant, fast-growing Chlorella vulgaris IPPAS C-1 cells, Algal Res. 49 (2020) 101881.

[41] A.W. Mayo, Effects of temperature and pH on the kinetic growth of unialga Chlorella vulgaris cultures containing bacteria, Water Environ. Res. 69 (1) (1997) 64–72, _eprint: https://onlinelibrary.wiley.com/doi/pdf/10.2175/106143097X125191.

[42] T.D. Brock, Life at high temperatures, Science 230 (4722) (1985) 132–138.

[43] Code of federal regulations, 2024, Safety and Health Regulations for Construction, Occupational Health and Environmental Controls.

[44] T. Huld, E. Paietta, P. Zangheri, I. Pinedo Pascua, Assembling typical meteorological year data sets for building energy performance using reanalysis and satellite-based data, Atmosphere 9 (2) (2018) 53, Number: 2 Publisher: Multidisciplinary Digital Publishing Institute.

[45] W.-C. Lin, C.-F. Tsai, Missing value imputation: a review and analysis of the literature (20062017), Artif. Intell. Rev. 53 (2) (2020) 1487–1509.

[46] F. Pedregosa, G. Varoquaux, A. Gramfort, V. Michel, B. Thirion, O. Grisel, M. Blondel, P. Prettenhofer, R. Weiss, V. Dubourg, J. Vanderplas, A. Passos, D. Cournapeau, M. Brucher, M. Perrot, E. Duchesnay, Scikit-learn: Machine learning in Python, J. Mach. Learn. Res. 12 (Oct) (2011) 2825–2830.

[47] G.Y. Lu, D.W. Wong, An adaptive inverse-distance weighting spatial interpolation technique, Comput. Geosci. 34 (9) (2008) 1044–1055.

[48] G.M. Sullivan, R. Feinn, Using effect sizeor why the p value is not enough, J. Grad. Med. Educ. 4 (3) (2012) 279–282.

[49] D. Yang, J.E. Dalton, A unified approach to measuring the effect size between two groups using SAS, in: SAS Global Forum, vol. 335, Citeseer, 2012, pp. 1–6.

[50] M. Ester, H.-P. Kriegel, J. Sander, X. Xu, A density-based algorithm for discovering clusters in large spatial databases with noise, vol. 96, 1996, pp. 226–231.

[51] A. Dai, T.R. Karl, B. Sun, K.E. Trenberth, Recent trends in cloudiness over the united states: A tale of monitoring inadequacies, Bull. Am. Meteorol. Soc. 87 (5) (2006) 597–606, Publisher: American Meteorological Society Section: Bulletin of the American Meteorological Society.

[52] D. Lambergeon, M. Leroy, L'automatisation de l'observation mètèorologique sur les aèrodromes français, La Mètèorologie (52) (2006) 18–27.

[53] H. Gulvanessian, J.-A. Calgaro, M. Holický, Designer's Guide to EN 1990: Eurocode: Basis of Structural Design, Thomas Telford, 2002, Google-Books-ID: 7Z8aMAHjyqQC.

[54] M. Mequignon, L. Adolphe, F. Thellier, H. Ait Haddou, Impact of the lifespan of building external walls on greenhouse gas index, Build. Environ. 59 (2013) 654–661.
[55] FishStatJ: Universal Software for Fishery Statistical Time Series, FAO Fisheries Division, 2020.
[56] B.M.E. Gerhard, K.A. Neil, P. Irina, Research for PECH committee - the future of the EU algae sector, 2023, Publisher: <bound method Organization.get_name_with_acronym of <Organization: European Parliamentary Research Service>>.
[57] R. Araújo, F. Vázquez Caldeórn, J. Sánchez López, I.C. Azevedo, A. Bruhn, S. Fluch, M. Garcia Tasende, F. Ghaderiardakani, T. Ilmjärv, M. Laurans, M. Mac Monagail, S. Mangini, C. Peteiro, C. Rebours, T. Stefansson, J. Ullmann, Current status of the algae production industry in Europe: An emerging sector of the blue bioeconomy, Front. Mar. Sci. 7 (2021) Publisher: Frontiers.
[58] M. Görs, R. Schumann, D. Hepperle, U. Karsten, Quality analysis of commercial Chlorella products used as dietary supplement in human nutrition, J. Appl. Phycol. 22 (3) (2010) 265–276.